Published in final edited form as:
Neurogastroenterol Motil. 2013 February ; 25(2): e89–e100. doi:10.1111/nmo.12057.

Visualization of spinal afferent innervation in the mouse colon by AAV8-mediated GFP expression

Daniel J. Schuster[1], **Jaclyn A. Dykstra**[2], **Maureen S. Riedl**[1], **Kelley F. Kitto**[1,3,4], **Christopher N. Honda**[1], **R. Scott McIvor**[5], **Carolyn A. Fairbanks**[1,3,4], and **Lucy Vulchanova**[6]

[1]Department of Neuroscience University of Minnesota, Minneapolis, MN 55455

[2]Comparative and Molecular Biosciences Graduate Program, College of Veterinary Medicine, University of Minnesota, Saint Paul, MN 55108

[3]Department of Pharmaceutics, University of Minnesota, Minneapolis, MN 55455

[4]Department of Pharmacology, University of Minnesota, Minneapolis, MN 55455

[5]Department of Genetics Cell Biology and Development, University of Minnesota, Minneapolis, MN 55455

[6]Department of Veterinary and Biomedical Sciences, University of Minnesota, Saint Paul, MN55108

Abstract

Background—Primary afferent neurons whose cell bodies reside in thoracolumbar and lumbosacral dorsal root ganglia (DRG) innervate colon and transmit sensory signals from colon to spinal cord under normal conditions and conditions of visceral hypersensitivity. Histologically, these extrinsic afferents cannot be differentiated from intrinsic fibers of enteric neurons because all known markers label neurons of both populations. Adeno-associated virus (AAV) vectors are capable of transducing DRG neurons after intrathecal administration. We hypothesized that AAV-driven overexpression of green fluorescent protein (GFP) in DRG would enable visualization of extrinsic spinal afferents in colon separately from enteric neurons.

Methods—Recombinant AAV serotype 8 (rAAV8) vector carrying the GFP gene was delivered via direct lumbar puncture. GFP labeling in DRG and colon was examined using immunohistochemistry.

Key Results—Analysis of colon from rAAV8-GFP treated mice demonstrated GFP-immunoreactivity (GFP-ir) within mesenteric nerves, smooth muscle layers, myenteric plexus, submucosa and mucosa, but not in cell bodies of enteric neurons. Notably, GFP-ir co-localized with CGRP and TRPV1 in mucosa, myenteric plexus, and globular-like clusters surrounding nuclei within myenteric ganglia. Additionally, GFP-positive fibers were observed in close association with blood vessels of mucosa and submucosa. Analysis of GFP-ir in thoracolumbar and lumbosacral DRG revealed that levels of expression in colon and L6 DRG appeared to be related.

CORRESPONDENCE: Lucy Vulchanova, Ph.D., Department of Veterinary and Biomedical Sciences, 295B AS/VM, 1988 Fitch Ave, St Paul, MN 55108, Phone: (612) 625-2731, Fax: (612) 625-0204, vulch001@umn.edu.

Author contributions: D.J.S.: experiments, data analysis, manuscript preparation; J.A.D.: experiments, data analysis; M.S.R.: experiments, manuscript preparation; K.F.K.: experiments; C.N.H: data interpretation and manuscript preparation; RSM: experimental design; CAF: experimental design, manuscript preparation, funding; L.V.: experimental design, data analysis and interpretation, manuscript preparation, funding.

Disclosures:
Competing interests: the authors have no competing interests.

Conclusions and Inferences—These results demonstrate the feasibility of gene transfer to mouse colonic spinal sensory neurons using intrathecal delivery of AAV vectors and the utility of this approach for histological analysis of spinal afferent nerve fibers within colon.

The colon is innervated by extrinsic primary afferent fibers whose cell bodies reside in thoracolumbar and lumbosacral dorsal root ganglia (DRG). These fibers transmit sensory information from the colon to the spinal cord under normal conditions and under conditions of visceral hypersensitivity. Functional analysis of the signaling mechanisms that underlie the responses of these sensory neurons has provided potential new drug targets for the management of abdominal pain and discomfort that accompany chronic gastrointestinal disorders such as irritable bowel syndrome (1–6).

Elucidation of the morphology and the anatomical localization of the extrinsic primary afferent nerves within the gut wall is integral to understanding their roles in visceral sensation. However, their morphological characterization has been hindered by the lack of markers that distinguish them from intrinsic fibers of the enteric nervous system. Intraganglionic injections of anterogtade tracers have been used for histological analyses of vagal afferents (7, 8), but the limited accessibility of DRG has precluded the application of this technique to spinal afferents. Visualization of extrinsic gut innervation has also been achieved by anterograde labeling *in vitro* (9–14) although the application of this technique to the analysis of colon afferents has been limited (11).

Targeted expression of fluorescent proteins in sensory ganglia through the generation of transgenic mouse lines or through viral vector-mediated gene transfer offers an alternative approach for morphological analysis of the extrinsic innervation of the gut wall (7, 15). Furthermore, viral vector-mediated gene transfer to visceral sensory neurons may enable functional validation of drug targets based on the overexpression or knockdown of genes of interest within sensory neurons (7). Adeno-associated virus (AAV) vectors have proven to be a valuable tool for such gene-transfer studies as many types of AAV are capable of producing long-term gene expression in primary sensory neurons (7, 16, 17). Targeted delivery, however, can be important as AAV vectors are capable of transduction in many types of neurons and non-nervous peripheral tissues as well (18–20). We have previously demonstrated that intrathecal administration of AAV vectors engineered to express green fluorescent protein (GFP) results in transduction of DRG neurons (17). The goal of the present study was to determine whether intrathecally administered AAV vector could achieve gene transfer to primary afferent sensory neurons innervating the colon without significant transduction of neuronal cells intrinsic to the colon. We hypothesized that GFP overexpression in primary afferent neurons would enable visualization of their peripheral processes in the colonic wall. Specifically, the gene for GFP was delivered to mouse DRG neurons by adeno-associated virus serotype 8 (rAAV8)-mediated gene transfer after direct lumbar puncture. Immunohistochemical analyses were conducted in DRG neurons and colonic nerves from rAAV8-GFP treated mice.

Methods

AAV Vector and Packaging

The AAV vector TRUF11, containing a CAGS-regulated GFP sequence, has been previously described (21). Packaging using an AAV8 serotype capsid was carried out at the University of Florida Vector Core Lab of the Gene Therapy Center (Gainesville, Florida) as previously described (21).

AAV Injections

All experiments were reviewed and approved by the Institutional Animal Care and Use Committee and the Institutional Biosafety Committee of the University of Minnesota. A 10 μL inoculum containing ~6–7 $\times 10^{10}$ viral particles was administered by intrathecal injection to conscious C57/Bl6 mice (20–25g b.wt.) as described previously (17, 22). Briefly, each animal was held gently at the iliac crest, and a 30 gauge, 0.5 inch needle connected to a 50 μL Hamilton syringe via a length of PE10 tubing was inserted between the 5^{th} and 6^{th} lumbar vertebrae for injection. To enhance transduction of DRG neurons (17, 23), mannitol (25% in 200 μL volume) was injected via the tail vein 20 min prior to vector administration. To attenuate the caudal to rostral diffusion of viral vectors, after the mannitol injection and prior to the intrathecal injection of rAAV8-GFP some mice were anesthetized (a mixture of 100 mg/kg ketamine, 20 mg/kg xylazine, 10 mg/kg acepromazine, i.p.) and positioned approximately vertically (head upward) by gently taping the paws of the animals to a mesh cage top, and propping the cage top on its side for the duration of anesthesia (approximately 1 h). Animals were monitored continuously for maintained respiration, and were returned to their home cage at the first sign of limb or head movement.

Immunohistochemistry

Tissues for immunohistochemical analysis were harvested from mice six weeks after vector injection or from naïve mice. Mice were overdosed with isoflurane and perfused transcardially with a solution of calcium-free Tyrodes solution (in mM: NaCl 116, KCl 5.4, $MgCl_2 \cdot 6H_2O$ 1.6, $MgSO_4 \cdot 7H_2O$ 0.4, NaH_2PO_4 1.4, glucose 5.6, and $NaHCO_3$ 26) followed by modified Zamboni's fixative (4% paraformaldehyde and 0.2% picric acid in 0.1M phosphate buffer, pH 6.9) followed by 10% sucrose in phosphate-buffered saline (PBS). In some cases, instead of perfusion-fixation segments of distal colon were immersion-fixed in the same fixative for 1 h at room temperature and then washed extensively in PBS. All tissues were stored in PBS containing 10% sucrose and 0.05% sodium azide until further use. Colon segments were sectioned transversely; however, in some specimens folding of the tissue near the end of the segments generated oblique sections that presented a nearly horizontal view of the tissue. Slide-mounted cryostat sections (14 or 20 μm thick) were incubated in blocking buffer (PBS containing 0.03% Triton X-100, 1% BSA, 1% normal donkey serum, 0.01% sodium azide) for 30 min at room temperature, followed by incubation in primary antisera overnight at 4°C. Primary antibodies used in these experiments included chicken anti-GFP (1:1000, Abcam, cat# 13970), rabbit anti-calcitonin gene related peptide (CGRP; 1:1000; ImmunoStar, Hudson WI, cat# 24112), rabbit anti-vasoactive intestinal peptide (VIP; 1:1000; ImmunoStar, Hudson WI, cat# 20077), rat anti-substance P (SP; 1:100; Oxford Biotechnology, UK), guinea pig anti-transient receptor potential vanilloid 1 (TRPV1; 1:500; ref. (24)), rabbit anti-smooth muscle actin (1:1000; Abcam, cat# 5694), and rat anti-CD31 (1:300; BD Pharmingen, cat# 557355). After rinsing with PBS, sections were incubated for one hour at room temperature with appropriate combinations of Cy2-, Cy3-, and Cy5- (1:300) conjugated secondary antisera (Jackson ImmunoResearch, West Grove, CA). Sections were rinsed again, and in some cases, were also incubated with 4′,6-diamidino-2-phenylindole (DAPI) nucleic acid stain for 3–5 minutes (300 nM; Invitrogen; Eugene, OR) or NeuroTrace (Invitrogen) according to manufacturer's instructions. Following the final rinses, sections were cover-slipped using glycerol and PBS containing 0.1% p-phenylenediamine (Sigma). Whole mount preparations: segments of colon from naive mice were opened longitudinally, pinned mucosal side down, fixed (1 h, room temp.), cleared (dehydration in alcohol series and xylene and rehydration), and dissected by removing first the mucosa/submucosa and then the circular muscle. Extended incubation and washing times were used for whole mount preparations and thick (100 μm) transverse sections: blocking buffer, overnight; primary antisera, approximately 36 h, secondary antisera, overnight; washing, 6–18 h.

Images were collected using an Olympus FluoView FV1000 confocal imaging system. Optical sections (slices) collected along the z-axis were projected using Image J. Pseudocolored multiple-labeling images were merged using Image J or Adobe Photoshop software and adjusted for contrast and brightness using Adobe Photoshop. Tissues from control mice that did not receive the GFP vector construct displayed no GFP-like immunofluorescence. In contrast, robust GFP fluorescence was seen in the cell bodies of DRG neurons from mice treated with the GFP construct (not shown). We chose to visualize GFP immunoreactivity (-ir) using indirect immunofluorescence in all experiments in order to maximize the detection of labeling in peripheral processes. There was substantial variability in the density of GFP-ir colonic fibers in specimens from different rAAV8-GFP treated mice (see Results). This latter observation suggests that the occurrence of "false-positive" immunofluorescence in these samples is highly unlikely.

Quantification of GFP expression in DRG

For each dorsal root ganglion, 5–8 non-overlapping images taken across 4–5 tissue sections, which were spaced by at least 56 μm, were used for analysis. Neurons were outlined based on NeuroTrace Nissl-like or background labeling, and only cells with a visible nucleus, identified by NeuroTrace or DAPI staining, were counted. GFP-ir fluorescence intensity measurements were obtained using Image J software. The intensity measurements of unlabeled cells were used to determine the labeling threshold for unbiased identification of GFP-positive neurons. For each ganglion the number of GFP-positive neurons was determined as a percentage of all neurons in the sampled sections. The data are expressed and Mean +/− Standard Error.

Results

Overview of GFP immunoreactivity in the colon and transduction of lumbosacral and thoracolumbar DRG

The localization of GFP-ir was examined in colon and DRG specimens six weeks after intrathecal administration of rAAV8-GFP to mice. GFP-ir was observed in mesenteric nerve bundles near the colon, a finding indicative of the extrinsic origin of GFP-positive nerve fibers (Fig. 1A). GFP-ir in the colonic wall was limited relative to the abundant intrinsic innervation illustrated by labeling for the neuropeptide substance P (SP) (Fig. 1A and 1B). The localization and density of GFP-ir fibers within the colon varied substantially between animals. In most colonic specimens GFP-ir was seen only in fibers in myenteric plexus or the submucosa, although in some cases numerous intensely labeled GFP-ir nerve fibers were also present throughout the submucosa, and the mucosa (Fig. 1C, 1D). Generally, GFP labeling was more abundant in the distal portion of the colon (approximately 1–3 cm from the anus) than in proximal portion (approximately 5–7 cm from the anus). In all experimental animals the intrinsic ganglia of the colon displayed no GFP labeling.

To evaluate the relationship between the presence of GFP-ir in colon and viral vector transduction in thoracolumbar and lumbosacral DRG, we determined the expression of GFP in L6, L5, L1, and T13 DRG of rAAV8-GFP treated mice (Fig. 2). In the experiment shown in Fig. 2A, the mean percentage of GFP-positive neurons increased rostrally in lumbar DRG, peaking in L1 DRG, and decreased dramatically in the adjacent T13 DRG. However, higher density of GFP labeling in colon corresponded to higher level of transduction in L6 DRG, and not L1 DRG. The transduction of L6 sensory neurons was augmented in mice that were anesthetized prior to the intrathecal administration of the vector and positioned approximately vertically (head upward) for the duration of the anesthesia (Fig. 2B and 2C).

GFP-positive nerve fibers in colonic myenteric plexus

To characterize the distribution of GFP-labeled fibers in the myenteric plexus, we examined their relationship relative to the neuropeptides substance P (SP) and calcitonin gene-related peptide (CGRP). Although some nerve fibers of extrinsic origin are SP-positive, SP-ir within the enteric nervous system is primarily associated with intrinsic neurons, and SP-positive nerve fibers are particularly abundant in the myenteric plexus. In contrast, a large proportion of the extrinsic sensory innervation of the mouse colon is CGRP-positive (25), whereas CGRP expression in intrinsic neurons is more limited than SP. In the myenteric plexus, GFP-ir fibers were observed in the nerve strands as well as within ganglia (Fig. 3 and 4). Most GFP-ir axons within the nerve strands were of fine caliber (Fig. 4 A–H), and instances of colocalization with CGRP- and SP-ir were evident (arrows in F and G). At high magnification, we observed axonal profiles that appeared to represent single large-diameter fibers rather than axon bundles (Fig. 4E, small arrows), although we cannot rule out the possiblility that these profiles correspond to bundles with nearly parallel trajectories. Within myenteric ganglia, GFP-ir profiles formed diffuse varicose networks (Fig. 3). GFP labeling in these networks overlapped extensively with CGRP-ir, but not with SP-ir. In addition to this diffuse branching pattern, we observed tightly intertwined, roughly globular, clusters of GFP-positive fibers that were intermingled with CGRP-positive fibers (Fig. 4, I–L, Fig. 5). The relationship of these clusters to SP-ir confirmed that they are located within myenteric ganglia (Fig. 4K). The clusters were most easily discernible in transverse sections. We considered the possibility that the clusters represent cross-sections of nerve strands in the myenteric plexus. Indeed, in instances where a nucleus was not present in the center of a cluster (not shown), it is likely that it corresponded to nerve strands passing through a ganglion. However, clusters surrounding nuclei labeled by DAPI within myenteric ganglia were also consistently observed (Fig. 4L, Fig. 5). GFP-ir and CGRP-ir overlapped partially in the clusters, indicating that they contained several intertwined fibers. Immunoreactivity for the transient receptor potential vanniloid type 1 ion channel (TRPV1-ir), which is involved in sensation of some nociceptoive signals, was similarly seen in fibers within the clusters (not shown). CGRP-ir clusters were also discernible in transverse colon sections from control mice in the absence of GFP labeling. Surprisingly, the clusters were not discernible in whole mount preparations from naïve mice, possibly because in the absence of GFP they were obscured by the dense CGRP-ir neuropil of the myenteric ganglia. Alternatively, analyses of thick transverse sections suggested that the clusters may be located near crossroads of nerve strands where the strands project though the circular muscle. Such a location is consistent with the apparent absence of the clusters in our whole mount preparations, in which the circular muscle was removed.

GFP-ir fibers in colonic mucosa and submucosa

GFP-ir fibers were frequently seen in close proximity to blood vessels in the mucosa and submucosa (Fig. 6A–D) which were visualized by the endothelial cell marker CD31. Individual fibers appeared to run parallel to blood vessels. This relationship was evident on circumferential blood vessels located adjacent to the circular muscle (Fig. 6C) and on mucosal vessels (Fig. 6B and D). In addition, there was evidence that GFP-ir fibers coil around blood vessels (arrows in 6A and 6B). GFP-ir innervation was also observed in ganglia of the submucosal plexus (Fig. 6F and G) as well as in the muscularis mucosa, a layer of smooth muscle underlining the lamina propria of the mucosa (Fig 6E). GFP-ir nerve bundles were seen coursing through the submucosal ganglia and towards the mucosa. Within the ganglia, there was also a fine network of GFP-ir innervation (Fig. 6F and G).

GFP-ir fibers in the mucosa were most frequently observed in the lamina propria surrounding the colonic crypts, but labeling was also present nearer the mucosal surface. GFP-ir colocalized with both CGRP-ir (Fig. 7A and B) and TRPV1-ir (Fig. 7C and D) in

mucosal fibers. However, the level of colocalization was often difficult to access due to intertwining of individual fibers and differences in the intensity of labeling of the different antibodies (Fig. 7A and D).

Discussion

The present study demonstrates the feasibility of gene transfer to spinal sensory neurons innervating mouse colon and offers a novel approach for histological analysis of their peripheral projections thoughout the different morphological layers of the gut wall. The minimally invasive administration of the viral vector by intrathecal injection allows access to lumbar DRG, which can be further restricted and enhanced by limiting diffusion of cerebrospinal fluid. Furthermore, there is evidence for differential targeting of subsets of sensory neurons by different AAV serotypes (17, 20, 26), suggesting that the utility of this approach for gene transfer and histological analysis can be further extended and refined by using different AAV vectors and reporter genes.

Our analysis of the relative contribution of lumbosacral and thoracolumbar DRG to GFP-ir in the colon suggests that the GFP-positive nerve fibers observed in the colonic wall originated from lumbosacral DRG. This conclusion is in agreement with previous work showing that the majority of sensory neurons retrogradely labeled from the murine colon are located within lumbosacral DRG (27, 28). The transduction of nodose ganglion neurons was not evaluated directly in the present study, but as GFP-ir was most abundant in nerve fibers within the distal colon, it is unlikely that nodose afferent fibers contributed significantly to them (29). Another potential source of GFP-ir fibers in colon are sympathetic postganglionic neurons within prevertebral ganglia. However, we observed no colocalization of GFP-ir with colonic nerve fibers displaying immunoreactivity for the norepinephrine synthetic enzyme dopamine *beta*-hydroxylase (data not shown). Therefore, viral transduction of sympathetic postganglionic neurons is unlikely. We conclude that the GFP-ir fibers observed in distal colon after intrathecal administration of rAAV8-GFP most likely originate from extrinsic primary afferent neurons within the lumbosacral DRG that project to the colon through pelvic (lumbosacral spinal) nerves. In addition to colon, it is likely that GFP-ir fibers would be present in other pelvic viscera such as the bladder or uterus as well as in somatic structures innervated by transduced DRG neurons. The limited transduction of T13 DRG neurons observed in this study is consistent with our previous observations of limited GFP labeling in thoracic spinal cord in contrast to abundant labeling not only at sacral and lumbar levels but also at cervical levels (17). Therefore, intrathecal delivery of AAV vectors may be less useful for labeling of the sensory innervation of structures whose primary afferent supply originates in thoracic ganglia.

The number of transduced neurons within lumbar DRG was highly variable among mice, but was markedly enhanced when the animals were maintained in a vertical position under anesthesia following the injection. The enhancement was most likely due to reducing the caudal-to-rostral flow of cerebrospinal fluid. In addition to cerebrospinal fluid flow, factors that may contribute to variable transduction include slight differences in the force, depth or angle of intrathecal injections. The density of GFP-ir fibers in colon was also quite variable between animals. Labeled fibers were observed most frequently in the myenteric plexus, whereas in the mucosa GFP-ir was seen only when the transduction level of L6 DRG neurons exceeded 15% of all neurons. This difference may be related to differential targeting of a subset of neurons by AAV8 as there is evidence that the tropism of AAV serotypes for sensory neurons varies (17, 20, 26). Furthermore, it is possible that in this study there was a preference for labeling of larger axonal profiles due to facilitated passive diffusion of GFP in their distal processes. GFP-ir in fibers colocalized substantially with

CGRP-ir, consistent with the neurochemical profile of retrogradely labeled extrinsic afferents (11, 25, 30).

Electrophysiological studies conducted *in vivo* and *in vitro* have identified several subtypes of mechanosensitive pelvic afferents (31–34). The mechanotransduction sites of these fibers within the wall of the colon are as yet poorly characterized. The varicose branching pattern of extrinsic parimary afferent fibers in myenteric ganglia has been previously observed (11). In experiments designed to assess the functional properties of these fibers, it was discovered that circumferential stretch and probing with von Frey filaments failed to activate afferent nerves in the tunica muscularis/myenteric plexus of guinea pig ileum and colon (11). These observations suggest that the varicose branching sensory fibers may be mechanically insensitive (31). Alternatively, these fibers may be activated by other types of mechanical stimuli that are difficult to simulate under *in vitro* conditions. In the submucosa, our observation of the close association of GFP-positive nerve fibers with the submucosal vasculature is consistent with evidence for mechanosensitivity of the sensory innervation of blood vessels (11, 14). In particular, nerve fibers located along circumferential blood vessels adjacent to the circular muscle layer (Fig. 6) appear to be positioned in a way that would enable detection of circumferential stretch of the gut wall.

An interesting finding in the present study is the observation of tightly intertwined globular clusters of primary afferent fibers surrounding cells within myenteric ganglia. The pattern of SP-ir in the vicinity of the clusters (Fig. 4) and the morphology of the nuclei (Fig. 4 and 5) suggest that the clusters surround myenteric neurons. A similar pattern of myenteric neuron encirclement by extrinsic nerves has been observed in the mouse jejunum (13). Although at present we cannot rule out the possibility that the clusters correspond to rectal intraganglionic laminar endings (rIGLE) previously described as transduction sites of distension-sensitive mechanoreceptors (9, 10), the two structures appear morphologically distinct: while the clusters are tightly packed around individual cells, the rIGLEs have branches that spread over a greater territory within the myeteric ganglia. Further studies are also necessary to determine the identity of myenteric neurons located within the clusters. One possibility is that these neurons may be Dogiel type II intrinsic primary afferent neurons. Such a relationship may allow extrinsic primary afferents to monitor and influence the activity of intrinsic primary afferent neurons. It is also possible that the extrinsic primary afferents are surrounding intrinsically mechanosensitive myenteric neurons (35–37), comprising a complex in which either or both components have mechanosensor properties. We speculate that the clusters illustrated in Fig. 4 and Fig. 5 represent sensory complexes within the myenteric plexus in which extrinsic sensory nerves may monitor and perhaps alter the mechanosensitivity of intrinsic neurons. In fact, the morphological appearance of these clusters is reminiscent of Meisner's corpuscles that mediate mechanosensation in the skin (38).

To our knowledge, this study reports the first visualization of extrinsic spinal nerve fibers in submucosal ganglia, muscularis mucosae, and mucosa of the colon. These fibers may belong to functional subtypes characterized as mucosal, muscular/mucosal or mechanically-insensitive afferents. It has been suggested that sensory fibers observed within the muscularis mucosae may represent anatomical substrates of spinal afferents with muscular/mucosal properties (32, 39). The spinal afferent innervation of submucosal ganglia could potentially contribute to vasomotor or secretory reflexes (40, 41). The observation of GFP-ir fibers in the mucosa is consistent with electrophysiologically-characterized pelvic mechanosensitive fibers that are classified as mucosal or muscular/mucosal and respond to mucosal stroking (31, 32). A proportion of mucosal and muscular/mucosal afferents are also sensitive to capsaicin (4), which is consistent with the partial overlap of GFP-ir and TRPV1-ir that we observed in these fibers. The mucosal GFP-ir fibers may also represent

chemosensing but mechanically insensitive afferents (31). The predominant localization of mucosal GFP-ir fibers in the crypt region may be due to limited GFP diffusion in the fine processes extending to the mucosal surface. Alternatively, the fibers in the crypt regions and near the surface might be attributable to the existence of different subtypes of sensory neurons with unique functional specializations. In the present study it was not possible to evaluate the extent to which a single fiber contributed to innervation of different structures within the gut wall.

In summary, we have performed a histological analysis of the extrinsic spinal afferents within mouse colon based on their anterograde labeling through rAAV8-directed expression of GFP in lumbar DRG neurons. This approach offers the potential for global visualization of the colonic spinal afferent innervation, its structural and neurochemical plasticity, and its relationship to other cellular components of the gut wall under normal conditions and in experimental models of visceral hypersensitivity. Integration of this methodology with the functional characterization of extrinsic afferents will enhance our understanding of the relationship of structure and function in the transduction and transmission of visceral afferent information.

Acknowledgments

Funding

The authors would like to thank Dr. David Brown for valuable discussions and manuscript review and Galina Kalyuzhnaya and Kelly Podetz-Pederson for technical assistance. The project was funded by NIH/NIDA (K01 DA017236, L.V. and CEBRA R21 DA025164, C.A.F.), NIH/NINDS (F31NS063634, D.J.S.), NIH T32 (RR18719, J.A.D.) and UMN Academic Health Center (C.A.F.).

ABBREVIATIONS

DRG	dorsal root ganglia
AAV	adeno-associated virus
GFP	green fluorescent protein
PBS	phosphate buffered saline
SP	Substance P
CGRP	calcitonin gene related peptide
VIP	vasoactive intestinal peptide
TRPV1	transient receptor potential vanniloid 1 receptor
-ir	immunoreactivity
MP	myenteric plexus
CM	circular muscle
LM	longitudinal muscle

References

1. Brenn D, Richter F, Schaible HG. Sensitization of unmyelinated sensory fibers of the joint nerve to mechanical stimuli by interleukin-6 in the rat: an inflammatory mechanism of joint pain. Arthritis Rheum. 2007; 56:351–359. [PubMed: 17195239]
2. Brierley SM, Hughes PA, Page AJ, et al. The Ion Channel TRPA1 Is Required for Normal Mechanosensation and Is Modulated by Algesic Stimuli. Gastroenterology. 2009

3. Brierley SM, Page AJ, Hughes PA, et al. Selective role for TRPV4 ion channels in visceral sensory pathways. Gastroenterology. 2008; 134:2059–2069. [PubMed: 18343379]
4. Jones RC 3rd, Xu L, Gebhart GF. The mechanosensitivity of mouse colon afferent fibers and their sensitization by inflammatory mediators require transient receptor potential vanilloid 1 and acid-sensing ion channel 3. J Neurosci. 2005; 25:10981–10989. [PubMed: 16306411]
5. La JH, Gebhart GF. Colitis decreases mechanosensitive K2P channel expression and function in mouse colon sensory neurons. American journal of physiology Gastrointestinal and liver physiology. 2011; 301:G165–174. [PubMed: 21512155]
6. Shinoda M, La JH, Bielefeldt K, Gebhart GF. Altered purinergic signaling in colorectal dorsal root ganglion neurons contributes to colorectal hypersensitivity. Journal of neurophysiology. 2010; 104:3113–3123. [PubMed: 20861433]
7. Kollarik M, Carr MJ, Ru F, et al. Transgene expression and effective gene silencing in vagal afferent neurons in vivo using recombinant adeno-associated virus vectors. The Journal of physiology. 2010; 588:4303–4315. [PubMed: 20736420]
8. Wang FB, Powley TL. Topographic inventories of vagal afferents in gastrointestinal muscle. The Journal of comparative neurology. 2000; 421:302–324. [PubMed: 10813789]
9. Lynn PA, Olsson C, Zagorodnyuk V, Costa M, Brookes SJ. Rectal intraganglionic laminar endings are transduction sites of extrinsic mechanoreceptors in the guinea pig rectum. Gastroenterology. 2003; 125:786–794. [PubMed: 12949724]
10. Olsson C, Costa M, Brookes SJ. Neurochemical characterization of extrinsic innervation of the guinea pig rectum. The Journal of comparative neurology. 2004; 470:357–371. [PubMed: 14961562]
11. Song X, Chen BN, Zagorodnyuk VP. Identification of medium/high-threshold extrinsic mechanosensitive afferent nerves to the gastrointestinal tract. Gastroenterology. 2009; 137:274–284. 284 e271. [PubMed: 19268671]
12. Spencer NJ, Kerrin A, Zagorodnyuk VP, et al. Identification of functional intramuscular rectal mechanoreceptors in aganglionic rectal smooth muscle from piebald lethal mice. American journal of physiology Gastrointestinal and liver physiology. 2008; 294:G855–867. [PubMed: 18218672]
13. Tan LL, Bornstein JC, Anderson CR. The neurochemistry and innervation patterns of extrinsic sensory and sympathetic nerves in the myenteric plexus of the C57Bl6 mouse jejunum. Neuroscience. 2010; 166:564–579. [PubMed: 20034545]
14. Zagorodnyuk VP, Brookes SJ, Spencer NJ. Structure-function relationship of sensory endings in the gut and bladder. Autonomic neuroscience: basic & clinical. 2010; 153:3–11.
15. Gautron L, Sakata I, Udit S, Zigman JM, Wood JN, Elmquist JK. Genetic tracing of Nav1. 8-expressing vagal afferents in the mouse. The Journal of comparative neurology. 2011; 519:3085–3101. [PubMed: 21618224]
16. Mason MR, Ehlert EM, Eggers R, et al. Comparison of AAV serotypes for gene delivery to dorsal root ganglion neurons. Mol Ther. 2010; 18:715–724. [PubMed: 20179682]
17. Vulchanova L, Schuster DJ, Belur LR, et al. Differential adeno-associated virus mediated gene transfer to sensory neurons following intrathecal delivery by direct lumbar puncture. Molecular pain. 2010; 6:31. [PubMed: 20509925]
18. Hartung SD, Frandsen JL, Pan D, et al. Correction of metabolic, craniofacial, and neurologic abnormalities in MPS I mice treated at birth with adeno-associated virus vector transducing the human alpha-L-iduronidase gene. Mol Ther. 2004; 9:866–875. [PubMed: 15194053]
19. Samaranch L, Salegio EA, San Sebastian W, et al. Adeno-associated virus serotype 9 transduction in the central nervous system of nonhuman primates. Hum Gene Ther. 2012; 23:382–389. [PubMed: 22201473]
20. Towne C, Pertin M, Beggah AT, Aebischer P, Decosterd I. Recombinant adeno-associated virus serotype 6 (rAAV2/6)-mediated gene transfer to nociceptive neurons through different routes of delivery. Molecular pain. 2009; 5:52. [PubMed: 19737386]
21. Kaemmerer WF, Reddy RG, Warlick CA, Hartung SD, McIvor RS, Low WC. In vivo transduction of cerebellar Purkinje cells using adeno-associated virus vectors. Mol Ther. 2000; 2:446–457. [PubMed: 11082318]

22. Hylden JL, Wilcox GL. Intrathecal morphine in mice: a new technique. European Journal of Pharmacology. 1980; 67:313–316. [PubMed: 6893963]
23. Fu H, Muenzer J, Samulski RJ, et al. Self-complementary adeno-associated virus serotype 2 vector: global distribution and broad dispersion of AAV-mediated transgene expression in mouse brain. Mol Ther. 2003; 8:911–917. [PubMed: 14664793]
24. Guo A, Vulchanova L, Wang J, Li X, Elde R. Immunocytochemical localization of the vanilloid receptor 1 (VR1): relationship to neuropeptides, the P2X3 purinoceptor and IB4 binding sites. The European journal of neuroscience. 1999; 11:946–958. [PubMed: 10103088]
25. Robinson DR, McNaughton PA, Evans ML, Hicks GA. Characterization of the primary spinal afferent innervation of the mouse colon using retrograde labelling. Neurogastroenterology and motility: the official journal of the European Gastrointestinal Motility Society. 2004; 16:113–124. [PubMed: 14764211]
26. Snyder BR, Gray SJ, Quach ET, et al. Comparison of adeno-associated viral vector serotypes for spinal cord and motor neuron gene delivery. Hum Gene Ther. 2011; 22:1129–1135. [PubMed: 21443428]
27. Christianson JA, Traub RJ, Davis BM. Differences in spinal distribution and neurochemical phenotype of colonic afferents in mouse and rat. J Comp Neurol. 2006; 494:246–259. [PubMed: 16320237]
28. Tan LL, Bornstein JC, Anderson CR. Distinct chemical classes of medium-sized transient receptor potential channel vanilloid 1-immunoreactive dorsal root ganglion neurons innervate the adult mouse jejunum and colon. Neuroscience. 2008; 156:334–343. [PubMed: 18706490]
29. Blackshaw LA, Gebhart GF. The pharmacology of gastrointestinal nociceptive pathways. Curr Opin Pharmacol. 2002; 2:642–649. [PubMed: 12482725]
30. Christianson JA, McIlwrath SL, Koerber HR, Davis BM. Transient receptor potential vanilloid 1-immunopositive neurons in the mouse are more prevalent within colon afferents compared to skin and muscle afferents. Neuroscience. 2006; 140:247–257. [PubMed: 16564640]
31. Feng B, Gebhart GF. Characterization of silent afferents in the pelvic and splanchnic innervations of the mouse colorectum. American journal of physiology Gastrointestinal and liver physiology. 2011; 300:G170–180. [PubMed: 21071510]
32. Brierley SM, Jones RC 3rd, Gebhart GF, Blackshaw LA. Splanchnic and pelvic mechanosensory afferents signal different qualities of colonic stimuli in mice. Gastroenterology. 2004; 127:166–178. [PubMed: 15236183]
33. Sengupta JN, Gebhart GF. Characterization of mechanosensitive pelvic nerve afferent fibers innervating the colon of the rat. J Neurophysiol. 1994; 71:2046–2060. [PubMed: 7931501]
34. Sengupta JN, Gebhart GF. The sensory innervation of the colon and its modulation. Curr Opin Gastroenterol. 1998; 14:15–20.
35. Mazzuoli G, Schemann M. Mechanosensitive enteric neurons in the myenteric plexus of the mouse intestine. PLoS One. 2012; 7:e39887. [PubMed: 22768317]
36. Schemann M, Mazzuoli G. Multifunctional mechanosensitive neurons in the enteric nervous system. Autonomic neuroscience: basic & clinical. 2010; 153:21–25.
37. Smith TK, Spencer NJ, Hennig GW, Dickson EJ. Recent advances in enteric neurobiology: mechanosensitive interneurons. Neurogastroenterology and motility: the official journal of the European Gastrointestinal Motility Society. 2007; 19:869–878. [PubMed: 17988274]
38. Pare M, Elde R, Mazurkiewicz JE, Smith AM, Rice FL. The Meissner corpuscle revised: a multiafferented mechanoreceptor with nociceptor immunochemical properties. The Journal of neuroscience: the official journal of the Society for Neuroscience. 2001; 21:7236–7246. [PubMed: 11549734]
39. Page AJ, Blackshaw LA. An in vitro study of the properties of vagal afferent fibres innervating the ferret oesophagus and stomach. The Journal of physiology. 1998; 512(Pt 3):907–916. [PubMed: 9769431]
40. Vanner S, Macnaughton WK. Submucosal secretomotor and vasodilator reflexes. Neurogastroenterology and motility: the official journal of the European Gastrointestinal Motility Society. 2004; 16(Suppl 1):39–43. [PubMed: 15066003]

41. Xue J, Askwith C, Javed NH, Cooke HJ. Autonomic nervous system and secretion across the intestinal mucosal surface. Auton Neurosci. 2007; 133:55–63. [PubMed: 17336595]

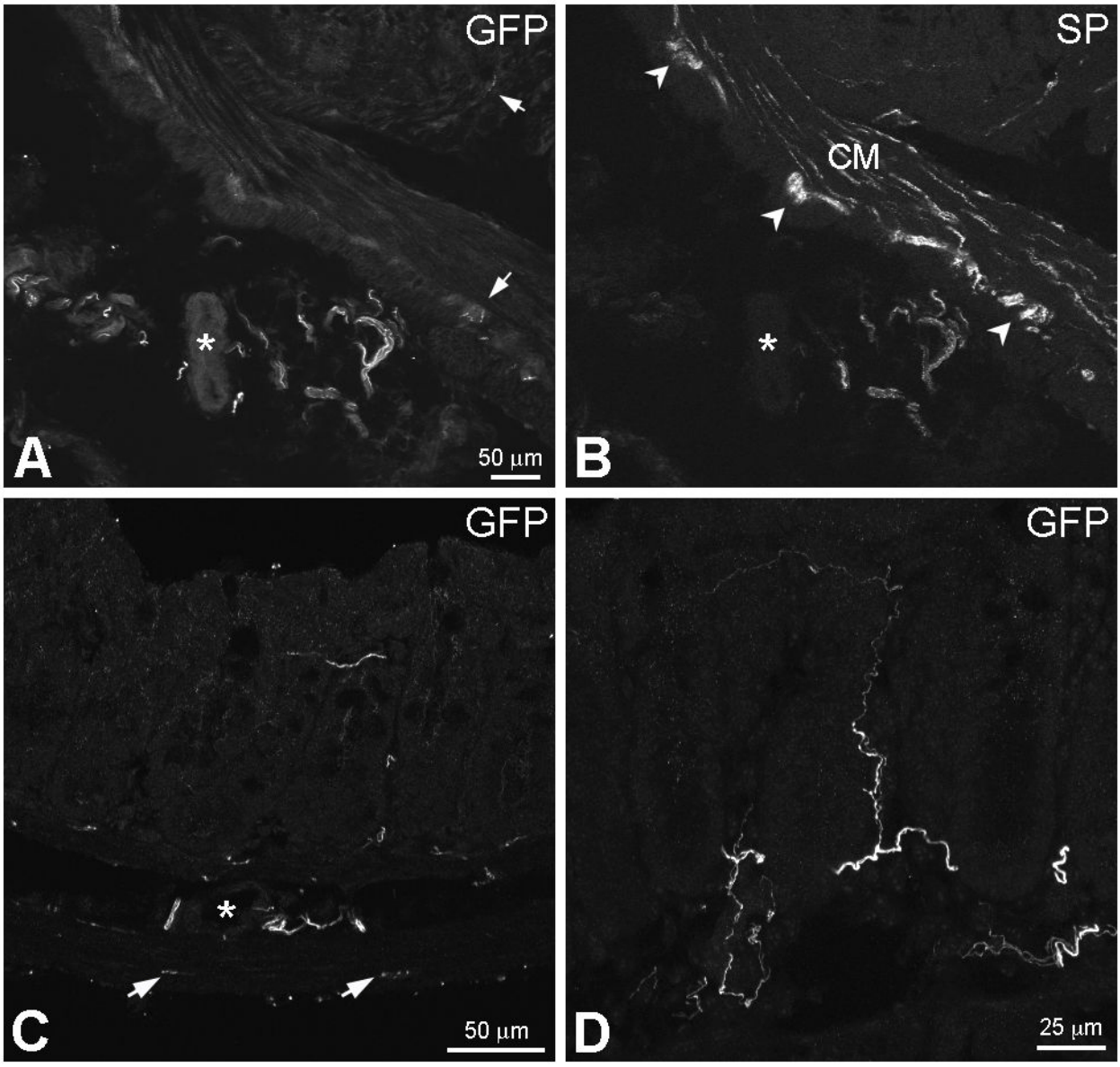

Figure 1.

Immunoreactivity to green fluorescent protein (GFP-ir) in mesenteric nerves and within the colonic wall. **A and B**, Double-labeling for GFP and SP. In A, GFP-immunoreactive (-ir) nerve bundles are present in the mesentery near a blood vessel (asterisks in A and B). GFP-ir fibers are also seen in the myenteric plexus (MP) and the mucosa (arrows). In B, extrinsic substance P (SP)-ir nerve fibers are present in mesenteric nerves. SP-ir of intrinsic origin is abundant in the colonic wall and delineates the MP (arrowheads) and circular muscle (CM). **C**, GFP-ir nerve fibers are present in the MP (arrows), the CM, the submucosa (asterisk indicates a submucosal blood vessel) and the mucosa. The image is a projection of 2 optical sections (slices) 2 μm apart. **D**, GFP-ir fibers within the mucosa (9 slices 2 μm apart). A fine fiber extends close to the mucosal surface (top of image). Scale bar: A–C, 50 μm; D, 25 μm.

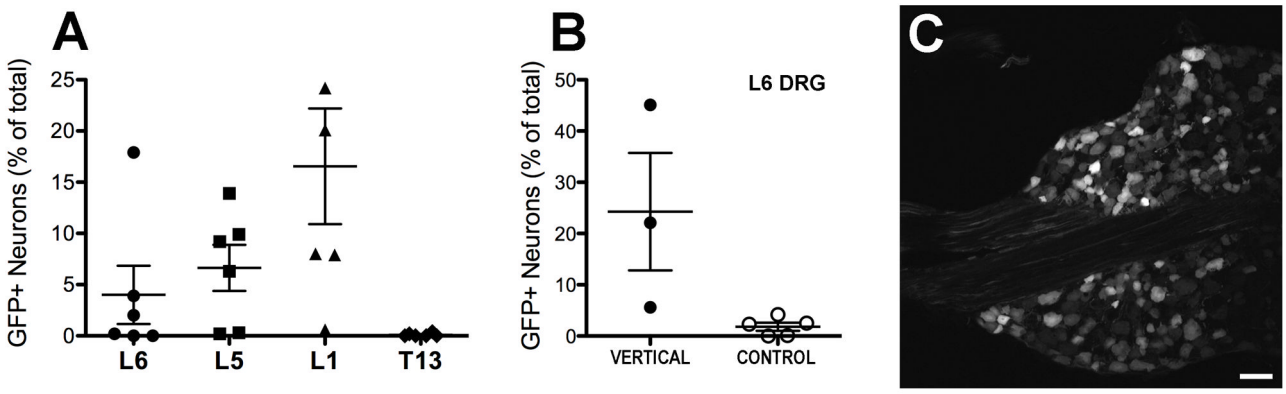

Figure 2.

Transduction of lumbosacral and thoracolumbar DRG by rAAV8-GFP after intrathecal vector delivery between the L5/L6 vertebrae. **A**, Gradient of transduction in lumbosacral (L5 and L6) and thoracolumbar (T13 and L1) DRG (n = 6; shown are mean +/− SE). **B**, Attenuation of caudal-to-rostral diffusion of cerbrospinal fluid increased transduction in L6 DRG (t-test, $P < 0.05$). The mice in group "VERTICAL" (n = 3) were injected intrathecally under anesthesia and positioned approximately vertically (head upward) for the duration of the anesthesia (approximately 1 h). The mice in group "CONTROL" (n = 5) were awake during the injection and allowed to move freely after it. **C**, Neuronal GFP-ir in the L6 DRG showing highest level of transduction in B. Scale bar: 50 μm.

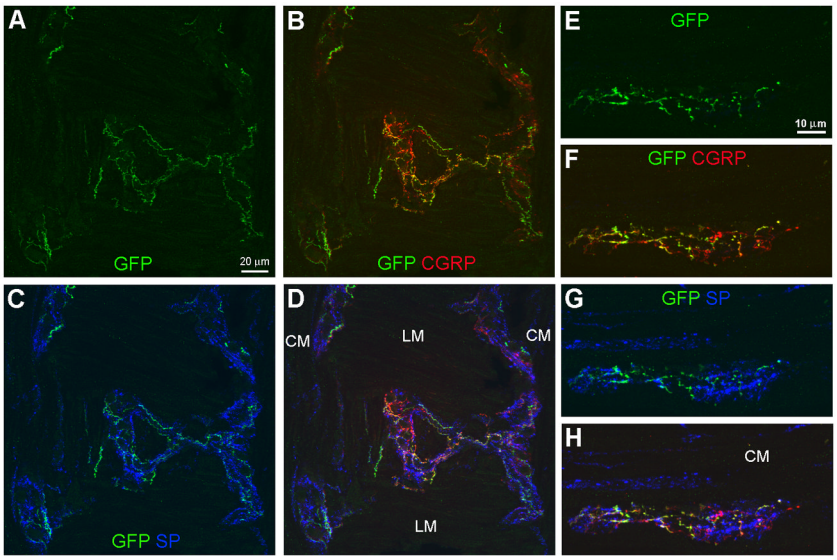

Figure 3.

GFP-ir varicose networks within the myenteric plexus. All images show GFP in green, CGRP in red, and SP in blue. **A–D**, Triple labeling for GFP, CGRP, and SP in a section through a folded region of the colon sample. Images (projections of 5 slices 1 μm apart) show a nearly horizontal view of the myenteric plexus overlaying the longitudinal muscle in the center and bordering the circular muscle (CM) at each side. **E–H**, Triple labeling for GFP, CGRP, and SP in a myenteric ganglion within a transverse colon section in which the CM is located above the ganglion. GFP-ir nerve fibers have a branching varicose appearance and form a diffuse network within the myenteric ganglia (A, E). GFP-ir overlaps substantially with CGRP-ir as indicated in B and F by the merging of green and red into orange and yellow. Colocalization of GFP- and SP-ir nerve fibers is limited (C, G). Scale bars: A–D, 20 μm; E–H, 10 μm.

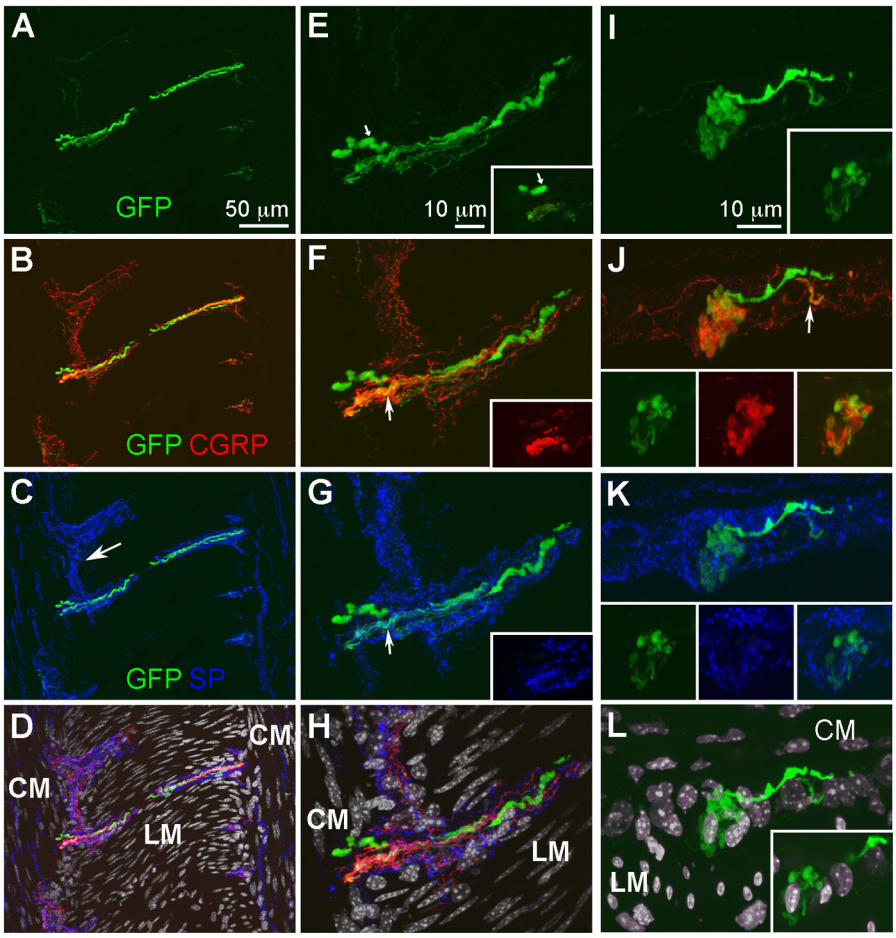

Figure 4.

GFP-ir fibers in a nerve strand and a globular cluster within the myenteric plexus. Images show triple labeling for GFP (green), CGRP (red), and SP (blue) with DAPI nuclear counterstain (gray) and are projections of 17 (A–D), 16 (E–H), or 12 (I–L) slices 1 μm apart. **A–D**, In a nearly horizontal section adjacent to the section displayed in Fig. 3, GFP-, CGRP-, and SP-positive fibers are seen in a nerve strand overlaying the longitudinal muscle (LM). Circular muscle (CM) and portions of myenteric ganglia (MG; arrow in C) are seen on each side of LM. **E–H**, A portion of the nerve strand in A–D shown at a higher magnification. Insets show a single slice from a region at the end of the nerve strand. In E, a single large axonal profile is indicated by small arrows. Colocalization of GFP-ir with CGRP- and SP-it is seen in some small –diameter axons (arrows in F and G). In D and H, the GFP-, CGRP-, and SP-positive fibers are shown relative to DAPI nuclear staining. Note the elongated nuclei of smooth muscle cells in the LM and CM oriented perpendicular to each other. Spherical nuclei are seen in the MG. **I–L**, A transverse section showing a globular cluster of GFP- and CGRP-ir fibers (I and J) within a MG that is demarcated by SP-ir (K). A single slice is shown in the insets. Two GFP-positive fibers appear to contribute to the cluster (I). The smaller of these fibers also shows CGRP-ir (see arrow in J). A single slice shown in the insets in J demonstrates that the cluster contains fibers that are double-labeled for GFP and CGRP as well as single-labeled GFP- and CGRP-ir fibers. The contribution of SP-ir fibers to the cluster is minimal (insets in K). In L, the GFP-ir cluster in shown relative to the nuclei of the LM and CM. Note that in the tranverse section nuclei of CM cells appear elongated, whereas LM nuclei are seen in cross-section. Nuclei of the MG

are seen between the layers of LM and CM nuclei. A single slice in the inset shows a nucleus in the center of the clustered fibers. Scale bars: A–D, 50 μm; E–L, 10 μm.

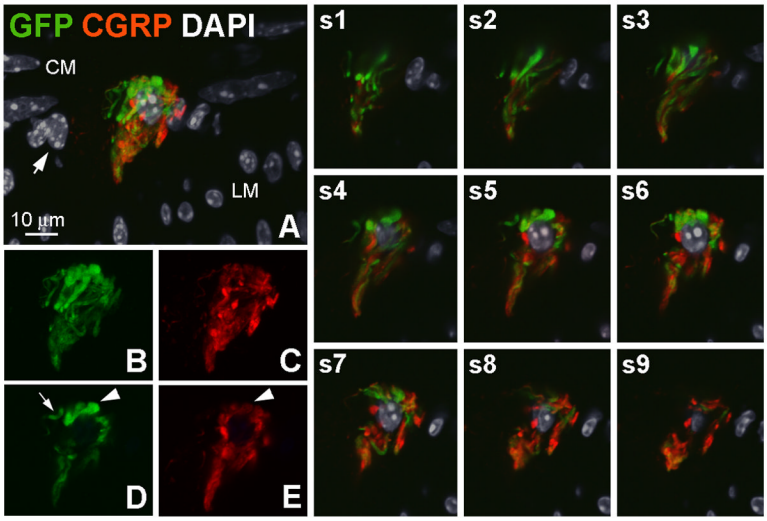

Figure 5.

A globular cluster of GFP-ir and CGRP-ir fibers. **A**, GFP- (green) and GCRP-positive (red) nerve fibers surrounding a nucleus labeled by DAPI (gray). DAPI-labeled small oval nuclei and elongated nuclei delineate the longitudinal and circular muscle layers, respectively. Nuclei located between these two layers (arrow), including the nucleus surrounded by nerve fibers, likely belong to neurons within a myenteric ganglion. The image is a projection of 9 slices 1 μm apart. **B–E**, Clusters of GFP- and CGRP-positive fibers are shown in B and C, respectively, (9 slices) and in a single slice (D and E). Arrowheads in D and E indicate a structure that is intensely GFP-positive and weakly CGRP-positive. The arrow in D indicates a segement of a fiber that is GFP-positive and CGRP-negative. Images s1–s9 show the relationship of GFP- and CGRP-ir fibers to the nucleus in the center of the cluster in individual optical sections. Scale bar: 10 μm.

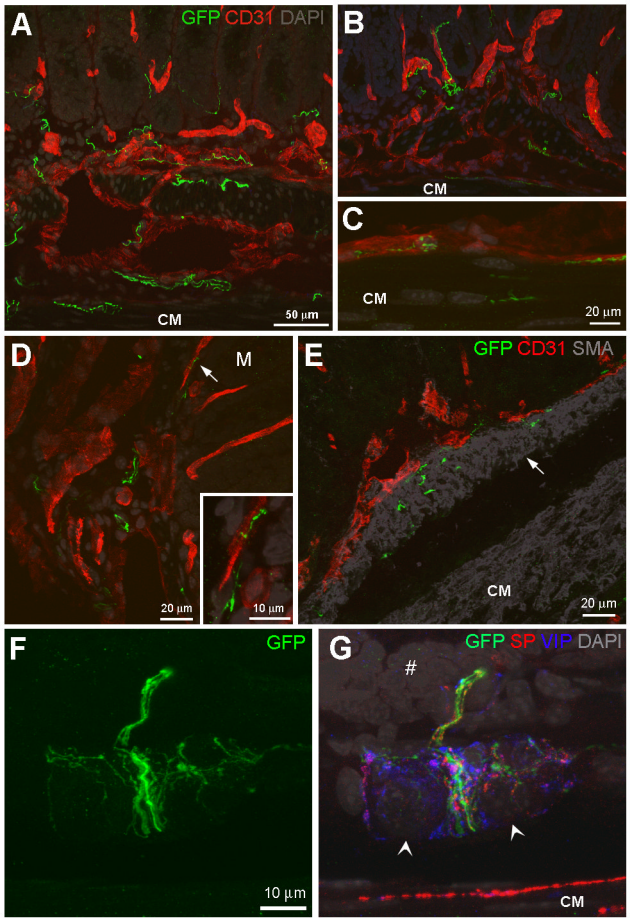

Figure 6.

Localization of GFP-ir fibers in the submucosa and mucosa of mouse colon. **A–D,** GFP-ir fibers (green) in circular muscle (CM), submucosa and mucosa. Blood vessels are visualized using the endothelial cell marker CD31 (red). DAPI labeling is shown in gray. **A and B,** GFP-ir fibers are frequently seen in close proximity to blood vessels in submucosa and mucosa (A, 7 slices 2 μm apart; B, 13 slices 1μm apart). Arrows indicate evidence of nerve fibers entwined around blood vessels. **C,** GFP-ir fibers are seen along a blood vessel adjacent to CM (9 slices 2 μm apart). **D,** GFP-ir nerve fibers in the submucosa and along a mucosal blood vessel (arrow) shown at higher magnification in the inset (D, 13 slices and inset 8 slices 1μm apart). The location of the mucosa is indicated by M. **E,** GFP-ir fibers in the muscularis mucosae (10 slices 1 μm apart), indicated by arrow, realtive to CD31 (red) and smooth muscle visualized using smooth muscle actin (SMA, gray). **F and G,** GFP-labeled fibers in a submucosal ganglion (14 slices 1 μm apart). **F,** A network of primary afferent innervation is seen within the gaglion and a bundle of nerve fibers of varying sizes courses through the ganglion towards the mucosa. **G,** The GFP-positive fibers are shown relative to SP- (red) and VIP-ir (blue) innervation of the ganglion, DAPI-labeled nuclei (likely to be neuronal; arrowheads), the CM and the crypt region of a mucosal fold (#). Scale bars: A and B, 50 μm; C–I, 20 μm; inset in D, 10 μm.

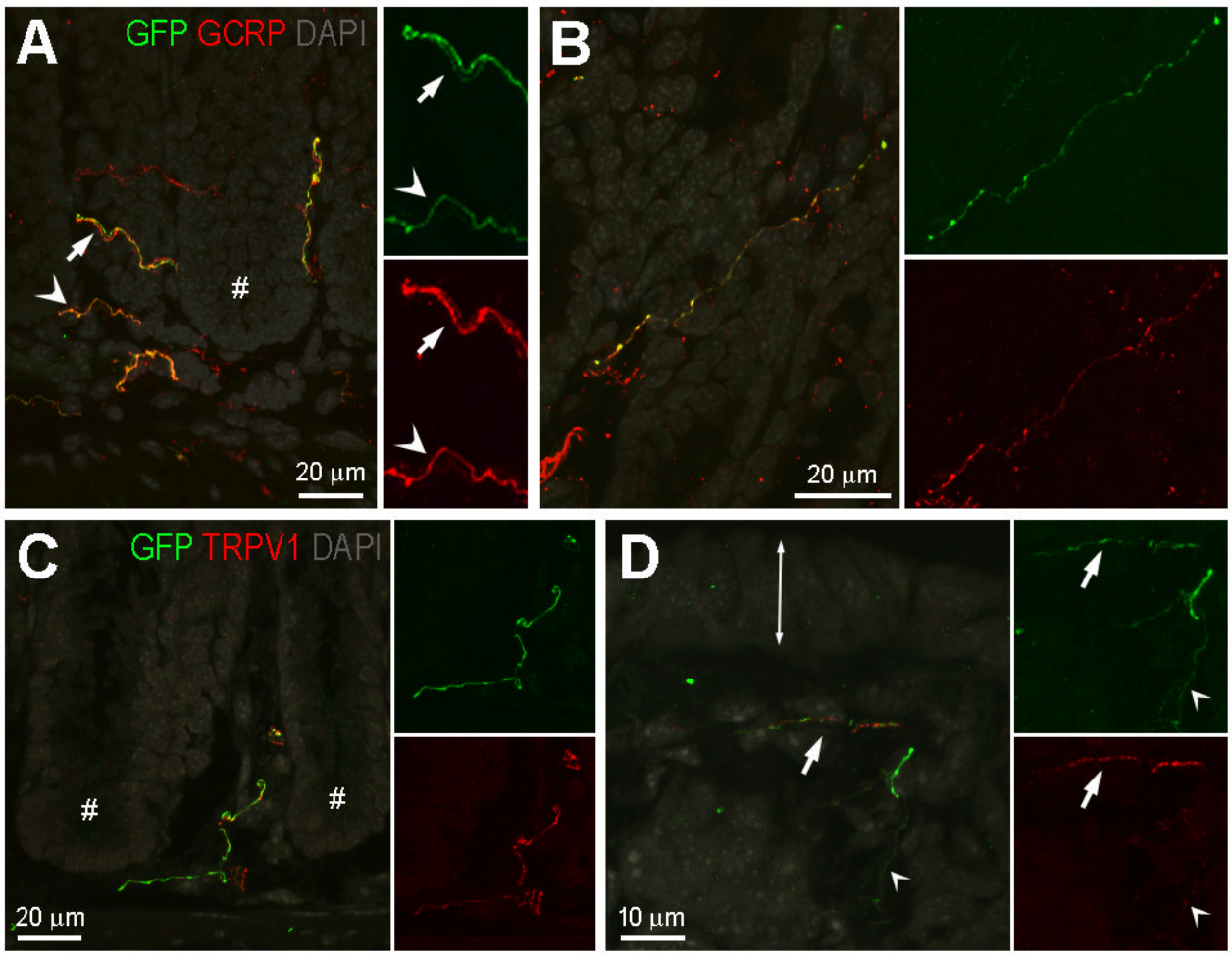

Figure 7.

GFP-ir nerve fibers in the colonic mucosa: relationship to CGRP-ir and TRPV1-ir. **A and B**, Relationship of GFP-ir (green) and CGRP-ir (red). DAPI labeling is shown in gray. Images are projections of 10 slices 1 μm apart. **A,** Colocalization of GFP- and CGRP-ir is indicated by orange hue in fibers (arrowheads); however in some cases in the merged pseudocolored image, intense labeling in one channel masks the labeling in the other channel creating the appearance of non-overlapping GFP-ir and CGRP-ir fibers (arrows). The single labeled insets are shown at doubled magnification to better illustrate fibers manifesting low intensity of labeling. Asterisk indicates the crypt region of a mucosal fold. **B,** A solitary nerve fiber immunoreactive for both GFP and CGRP in an oblique section through the mucosa. **C and D,** Relationship of GFP-ir (green) and TRPV1-ir (red). DAPI labeling is shown in gray. **C,** A nerve fiber immunoreactive for both GFP and TRPV1 in the crypt region of the mucosa (crypts indicated by #). TRPV1-positive/GFP-negative fibers are also present. **D,** Nerve fibers near the mucosal surface (double-ended arrow indicates the location of the epithelium at the mucosal surface). The alternating appearance of GFP- and TRPV1-ir suggests that two separate fibers are intertwined (arrow). Colocalization may exist in the fine-caliber fiber (arrowhead). Scale bars: A, 20 μm relative to A and 10 μm relative to insets; B and C, 20 μm; D, 10 μm.